CHEMISTRY OF MATERIALS

Article

pubs.acs.org/cm

Family of Single-Micelle-Templated Organosilica Hollow Nanospheres and Nanotubes Synthesized through Adjustment of Organosilica/Surfactant Ratio

Manik Mandal[†,‡,§] and Michal Kruk*[,†,‡]

[†]Center for Engineered Polymeric Materials, Department of Chemistry, College of Staten Island, City University of New York, 2800 Victory Boulevard, Staten Island, New York 10314, United States

[‡]Graduate Center, City University of New York, 365 Fifth Avenue, New York, New York 10016, United States

Supporting Information

ABSTRACT: A family of hollow organosilica nanospheres and nanotubes was synthesized at appropriately low organosilica-precursor/block-copolymer-surfactant ratios. In Pluronic F127 ($EO_{106}PO_{70}EO_{106}$) block copolymer templated synthesis of ethylene-bridged organosilicas in the presence of a swelling agent, the lowering of the organosilica-precursor/surfactant ratio led to a change from highly ordered face-centered cubic structure of spherical mesopores to individual hollow spherical nanoparticles. It was hypothesized that at low ratios of organosilica precursor to PEO-PPO-PEO, the framework precursor is solubilized in the micelles and its concentration on their surface is not sufficient to induce appreciable cross-linking between the resulting nanoobjects and the consolidation into larger particles. The inner pore size of the nanospheres was adjusted by varying the micelle expander, allowing us to obtain pore diameters up to ~20 nm. By employing low precursor/surfactant ratios, hollow spheres of methylene-, ethenylene-, and phenylene-bridged organosilicas were synthesized. Hollow silica spheres were also obtained through judicious choice of block copolymer. The synthesis strategy involving the adjustment of the framework-precursor/surfactant ratio was further extended on organosilica nanotubes synthesized using Pluronic P123 surfactant and cyclohexane as a swelling agent. One can envision a large number of framework compositions for which hollow nanospheres and nanotubes can be obtained using our synthesis approach.

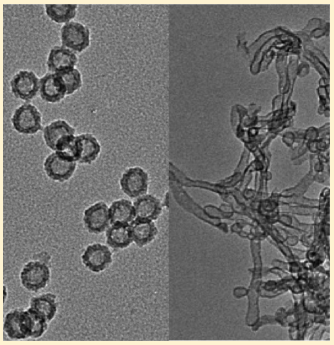

KEYWORDS: *organosilica, nanosphere, nanotube, pore size adjustment, periodic mesoporous organosilica*

INTRODUCTION

Surfactants are known from the ability of their molecules to form micelles of uniform size (typically in the range from several to several tens of nanometers) and well-defined shape (for instance, spherical and cylindrical).[1,2] The micelles can further aggregate[1] forming lyotropic liquid crystal structures, such as ordered arrays of cylinders or spheres. In the early 1990s, we have witnessed the emergence of a new family of nanoporous materials synthesized through surfactant-templating mechanism.[3−8] The synthesis involves the formation of silica/surfactant nanocomposites (or generally solid-framework/surfactant nanocomposites, where the framework-forming compound can be of inorganic, organic, or hybrid organic−inorganic nature[9−12]) upon addition of an appropriate precursor to the surfactant solution. The composites are composed of surfactant micelles encapsulated in the framework formed by the other component. Initially, it was envisioned that a preformed liquid-crystalline phase of surfactant micelles serves as a template for the formation of these nanoscale composites.[8] Later, it was shown that the formation of silica−surfactant composites typically involves self-assembly of silica precursor and the surfactant unimers into ordered nanoscale composites.[5,6]

In the late 1990s, oligomer and block-copolymer surfactants with poly(ethylene oxide) (PEO) units were found to be highly attractive alternatives[7,13−15] of alkylammonium and neutral amine surfactants[3,4,8,16] in the micelle-templated synthesis of mesoporous silicas and other compositions. Pluronic poly(ethylene oxide)-poly(propylene oxide)-poly(ethylene oxide) (PEO-PPO-PEO) triblock copolymers are a prominent family of the PEO-based surfactants.[1,17,18] PEO-PPO-PEO surfactant molecules feature hydrophilic PEO blocks and hydrophobic PPO block. In aqueous solutions, PPO blocks form a core of the micelle, while PEO blocks form a hydrated corona around the core. The interactions of PEO-based surfactants with the silica and organosilica framework precursors were found to involve the formation of the framework around the PEO chains in the corona of the micelle.[19,20] This finding was used to explain the existence of micropores in the walls of block-copolymer-templated ordered mesoporous silicas, including a two-dimensional hexagonal structure known as SBA-15 silica.[21] Because of the fact that the condensation of the framework precursor takes place in the proximity of the PEO chains, but

Received: July 25, 2011
Revised: November 30, 2011
Published: December 4, 2011

without any covalent or direct ionic interactions between the PEO chains and the framework, the proportion of the framework-forming compound to PEO-based surfactant can vary to an appreciable extent without changing the structure type of the resulting composite.[22,23] However, a significant excess of the silica precursor (tetraethyl orthosilicate, TEOS) results in the development of constrictions (plugs) in the mesopores of the silica material,[24] which was attributed to the solubilization of the excess of the hydrophobic TEOS in the hydrophobic cores of the micelles.[22] The effect of the low ratio of the framework precursor to surfactant was considered as a cause of the pore wall thinning.[23]

Recently, there has been a lot of interest in the synthesis of silica-based hollow nanoparticles, such as nanospheres and nanotubes, because of their exciting nanoscale architectures and prospects of their use as drug delivery media and contrast agents.[25−48] One of the approaches that has emerged for the synthesis of hollow silica,[26,29,33,34,47,49] organosilica,[27,50] and surface-functionalized organosilica[51,52] particles on the ten-of-nanometers length scale was the single micelle templating, allowing one to obtain spherical particles,[26,27,29,32−34,49−58] and, in some cases, nanotube-like particles.[28,48,59−61] The formation of these nanostructures was achieved through a selection of a particular block copolymer template (for instance, Pluronic F127[27,29,32,49−52,55,57,58] or F108[33,56] or P123[59−61]) and conditions (addition of appropriate inorganic salt[29] or acid,[61] copolymer surfactant concentration[60] or temperature[33]). There arises a question as to why these conditions led to individual particles, while the surfactants normally interact with silica (or organosilica) sources to form consolidated structures, such as ordered mesoporous silicas (or organosilicas) under similar conditions. In some cases, individual particles were stabilized using an agent that would suppress cross-linking between the particles.[32,56−59] Only in two cases, there emerged a theme that isolated particles form at lower silica−surfactant ratio while a larger relative amount of surfactant leads to the formation of consolidated structures,[33,34] but the transition was documented for silicas only and based solely on using transmission electron microscopy (TEM). The transition from consolidated structures to individual particles induced by the change in the framework-precursor/copolymer−surfactant ratio has not been reported for organosilicas.

Recently, we studied[62−65] the use of Pluronics as templates for the synthesis of ordered mesoporous organosilicas with organic groups integrated in the silica-based frameworks.[11,66−72] These organosilicas were synthesized using bis(trialkoxysilyl)organic precursors, where the organic bridging group was a short aliphatic (methylene, $-CH_2-$, ethylene, $-CH_2-CH_2-$) group, unsaturated chain (ethenylene, $-CH=CH-$), or aromatic ring (phenylene, $-C_6H_4-$). Under some conditions when bis(triethoxysilyl)ethane was used, ethylene-bridged organosilicas exhibited structures with poor periodicity and very rough surfaces, which seemed to be composed of hollow nanoparticles of fairly uniform size.[65] Subsequently, as described herein, we have documented[73] a transition from consolidated mesoporous ethylene-bridged organosilica structures of face-centered cubic symmetry (similar to those already reported by others and us)[63,72] templated by Pluronic F127 to very uniform individual and aggregated hollow spherical particles (for instance similar to those reported recently by others[27,49]). The transition from consolidated structures to individual nanospheres was triggered by the decrease in the amount of the organosilica precursor relative to the amount of the triblock copolymer template. We hypothesized that one can obtain hollow organosilica nanoparticles of different framework compositions using low organosilica-precursor/copolymer−surfactant ratios, and, indeed, we were able to obtain hollow spherical organosilica structures with methylene, ethenylene, and phenylene bridging groups.[73] Our strategy was extended on organosilica nanotubes with large mesopores (>10 nm),[73] which complements recent work by others on their smaller-pore counterparts.[60]

EXPERIMENTAL SECTION

Synthesis of Ethylene-Bridged Organosilica Hollow Nanospheres. The synthesis was carried out in the way similar to our earlier study of face-centered cubic PMOs,[63] but with variable precursor/surfactant ratio (instead of a fixed ratio of 2.90 g of bis(trimethoxysilyl)ethane (BTME) per 0.50 g F127) and somewhat higher stirring speed. More specifically, 0.50 g of Pluronic F127 ($EO_{106}PO_{70}EO_{106}$) was dissolved in 30 g of 2.0 M HCl solution under mechanical stirring at 15 °C. It should be noted that the mixture was prepared in a polypropylene (PP) bottle with its mouth taped with parafilm leaving a hole for the stirrer. Then, 0.50 g of 1,3,5-trimethylbenzene (TMB) and 2.50 g of KCl was added. After two hours, a selected mass of BTME (0.80, 1.00, 1.40, 2.00, 2.30, 2.60, 2.90, or 3.20 g) was added. The reaction mixture was mechanically stirred for 1 day at 15 °C (in a PP bottle with taped mouth). Subsequently, the mixture was heated at 100 °C for 1 day in a closed PP bottle. The as-synthesized material was filtered, washed with deionized water, and dried at ∼60 °C in a vacuum oven. Then, the surfactant was removed through the Soxhlet extraction with ethanol.

Synthesis of Large-Pore Ethylene-Bridged Organosilica Hollow Nanospheres. The synthesis was similar to that described above, but the mass of BTME was 0.99 g, no salt was added, magnetic stirring in a covered container, and toluene (or benzene) (0.50 g) were used. After the low-temperature step, the reaction mixture was treated hydrothermally at 100 °C for 1 d.

Synthesis of Methylene-Bridged Organosilica Hollow Nanospheres. The synthesis was similar to that reported for consolidated, weakly ordered PMO,[62] but with bis(triethoxysilyl)methane (BTEM)/F127 ratio reduced to 49% of original value. Also, TMB was replaced with xylenes (mixture of isomers), following our work on consolidated structures.[63,74] Specifically, 0.50 g of Pluronic F127 was dissolved in 45 mL of 2.0 M HCl solution under magnetic stirring at 15 °C in a covered container. Subsequently, 0.50 g of xylenes and 2.5 g of KCl were added, and, after 2 h, 1.03 mL of BTEM was introduced. The solution was stirred for 1 day at 15 °C, and later the reaction mixture was hydrothermally treated at 100 °C for 1 d. The resulting as-synthesized material was isolated as described above. Finally, the sample was calcined under N_2 at 300 °C for 5 h with heating ramp 2 °C/min.

Synthesis of Ethenylene-Bridged Organosilica Hollow Nanospheres. 0.50 g of Pluronic F127 was dissolved in 30 g of 2 M HCl under magnetic stirring at 15 °C. Subsequently, 0.50 g of xylenes and 2.50 g of KCl were added. After 2 h, 0.83 g of bis(triethoxysilyl)-ethylene (BTEEn) was introduced. The solution was kept under magnetic stirring in a covered container for 1 d and hydrothermally treated at 100 °C for 1 d in a closed container. After filtering, washing, and drying, the surfactant was removed through the Soxhlet extraction with ethanol.

Synthesis of Phenylene-Bridged Organosilica Hollow Nanospheres. The synthesis was similar to that described for ethenylene-bridged organosilica, but 0.93 mL of bis(triethoxysilyl)benzene (BTEB) was used as a framework precursor and as-synthesized material was calcined under nitrogen at 300 °C for 5 h to remove the surfactant.

Synthesis of Silica Nanospheres Using Pluronic F108. 0.50 g of Pluronic F108 ($EO_{132}PO_{50}EO_{132}$, BASF) was dissolved in 30.8 mL of 1.97 M HCl under magnetic stirring at 15 °C. After one hour, 0.61 g of xylenes and 2.5 g of KCl were added. After 2 h, 0.70 g of tetraethylorthosilicate (TEOS) was introduced. The mixture was

dx.doi.org/10.1021/cm202136r | Chem. Mater. 2012, 24, 123−132

stirred for 1 d in a covered container and subsequently hydrothermally treated at 100 °C for 2 d. The as-synthesized material was isolated as described above. Finally, the as-synthesized sample was calcined under air at 550 °C for 5 h with heating ramp 2 °C/min.

Synthesis of Ethylene-Bridged Organosilica Nanotubes. The synthesis was similar to that reported earlier for 2-D hexagonal ethylene-bridged PMO,[64] but bis(triethoxysilyl)ethane (BTEE) was used as a precursor instead of BTME, the precursor/F127 ratio was 46% lower than the lowest one used therein, and NH_4F was added. Specifically, 1.2 g of Pluronic P123 was dissolved in 42 mL of 1.3 M HCl solution under mechanical stirring at 15 °C. After 3 h, 0.014 g of NH_4F was added. After 1 h, a mixture of 2.18 g of BTEE and 5.0 g of cyclohexane was added. The reaction mixture was stirred for 1 d and subsequently hydrothermally treated at 100 °C for 2 d. The as-synthesized material was isolated as described above. Finally, the surfactant was removed from the material via Soxhlet extraction with ethanol.

Measurements. Small-angle X-ray scattering (SAXS) patterns were recorded on Bruker Nanostar U instrument equipped with Cu K_α radiation source (rotating anode operated at 50 kV, 24 mA). Samples were placed in a hole of an aluminum sample holder and secured on both sides with a Kapton tape. Nitrogen adsorption measurements were performed on Micromeritics ASAP 2020 volumetric adsorption analyzer at −196 °C. The samples were outgassed at 140 °C in the port of the adsorption analyzer before analysis. TEM images were taken on FEI Tecnai Spirit microscope operated at an accelerating voltage of 120 kV. Before the imaging, the samples were sonicated in ethanol and then were drop-casted on a carbon coated copper grid, and the solvent was allowed to evaporate under air. Weight change patterns were recorded under air using Hi-Res 2950 thermogravimetric analyzer from TA Instruments.

Calculations. The BET specific surface area (S_{BET}) was determined from nitrogen adsorption isotherm in the relative pressure from 0.04−0.2.[75] Total pore volume (V_t) was estimated from the amount adsorbed at a relative pressure of 0.99.[75] Pore size distributions (PSDs) were calculated from adsorption branches of the isotherms using the Barrett−Joyner−Halenda (BJH) method[76] with KJS correction for cylindrical mesopores.[77] It was shown[78,79] (based on eq 10 reported by others[80]) that this method underestimates the diameter of spherical mesopores of the size considered herein by ∼3 nm. The micropore volume (V_{mic}) was calculated using the α_s plot method in the standard reduced adsorption range of 0.9−1.2.[81] In the α_s method, LiChrospher Si-1000 was used as a reference.[81]

RESULTS AND DISCUSSION

A series of ethylene-bridged organosilicas was synthesized using Pluronic F127 as a surfactant, TMB as a micelle swelling agent, and different amounts of BTME as a framework precursor. Organosilicas synthesized with a higher relative amount of BTME (2.0−3.2 g BTME per 0.5 g F127) exhibited SAXS patterns (Figure 1) characteristic of face-centered cubic structure, which was highly ordered except for the lowest of the considered amounts of BTME. A similar material has been prepared earlier[63] using 2.9 g of BTME per 0.50 g of F127, and a somewhat slower stirring rate, which resulted in a somewhat larger unit-cell size. As the relative proportion of BTME decreased, SAXS patterns became less well resolved, featuring two or more broad peaks (see cases of 0.8 and 1 g of BTME). TEM (Figure 2) showed that these organosilicas were composed of uniform spheres with hollow interiors, whereas the organosilicas prepared with high proportions of BTME were consolidated periodic structures. The synthesis with 1.4 g BTME afforded a material that was intermediate, that is, the structure was not periodic but aggregated to a significant extent. The latter BTME/F127 ratio is similar to that used by others in

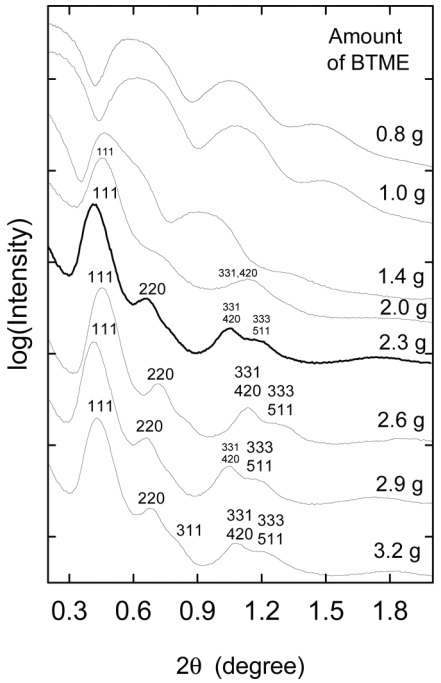

Figure 1. SAXS patterns for ethylene-bridged organosilicas synthesized with different relative amounts of BTME.[73]

their study of hollow spheres using a similar synthesis gel composition,[49] but other conditions were slightly different.

Shown in Figure 3 are nitrogen adsorption isotherms for the considered series of samples and the corresponding specific surface areas, total pore volumes, micropore volumes, and pore diameters are listed in Supporting Information Table S1. The materials obtained at the highest proportions of BTME (2−3.2 g) exhibited isotherms characteristic of periodic mesoporous organosilicas (PMOs) with spherical mesopores of large, uniform size.[63] The mesopores were accessible through narrow entrances, as seen from desorption at the lower limit of adsorption−desorption hysteresis, that is, p/p_0 = ∼0.48.[63] Previous studies documented such materials, and indeed the conditions used herein were similar to those reported earlier in the case of PMO synthesis.[63,72] On the other hand, the samples prepared with lower BTME/F127 ratios exhibited a prominent uptake of nitrogen at relative pressures above the capillary condensation pressure (p/p_0 = ∼0.83) related to the uniform mesopores. On the basis of TEM images, whose examples were discussed above, and of the previously reported studies,[27,29,49] the significant uptake close to the saturation vapor pressure can be attributed to capillary condensation between the loosely arranged spherical particles of the materials. The combination of TEM and gas adsorption data clearly shows a transition between the consolidated, highly ordered Fm3m structure of mesopores, and individual (or somewhat aggregated) hollow nanospheres as the proportion of the framework precursor to the surfactant is lowered. Only one similar transition has been documented for ordered mesoporous materials, namely silicas, but this one involved an intermediate structure of face-centered cubic array of hollow spheres,[33] which was not seen in the current study for organosilicas (no porosity arising from tetrahedral or octahedral holes can be identified based on TEM and adsorption). The other study reported transition between a disordered consolidated porous silica and isolated spheres.[34]

dx.doi.org/10.1021/cm202136r | Chem. Mater. 2012, 24, 123−132

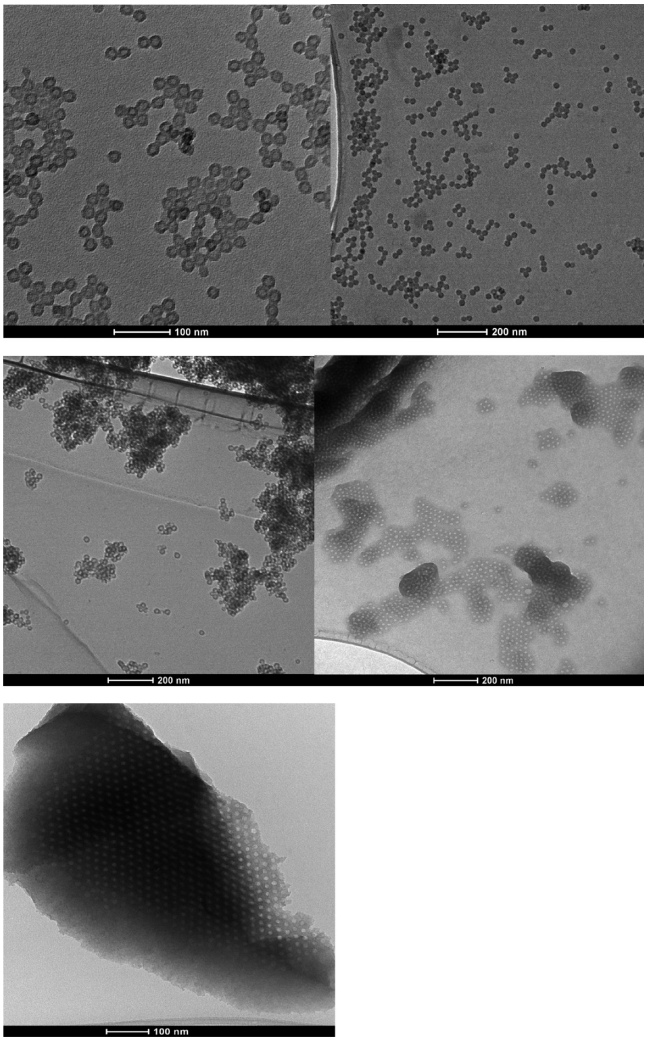

Figure 2. TEM images for the ethylene-bridged organosilicas prepared with different amounts of BTME precursor per 0.50 g F127: 0.8 g (top left), 1.0 g (top right), 1.4 g (middle left), and 2.0 g (middle right), and 3.2 g (bottom).[73]

Pore size distributions (PSDs) of all the materials were narrow and centered at ~13 nm (see Supporting Information Table S1 and Figure 4 for PSDs of materials prepared with lower BTME/F127 ratios; the behavior of the other materials, which are PMOs, is analogous to that discussed elsewhere[63]). The similarity of the mesopore size indicated that similar micelles templated the uniform mesopores in both consolidated materials and individual nanospheres. It can be inferred that each spherical mesopore is templated by a single micelle,[32] otherwise it is difficult to explain the uniform size and shape of the mesopores visible by TEM and probed by gas adsorption. In addition, the samples prepared with low BTME/F127 ratio exhibited a significant fraction of larger pores, whose distributions were broad (but exhibited maxima at ~25−30 nm in some cases).[49] The larger pores were not uniform in size, as expected for pores formed between nonuniformly packed particles. The replacement of TMB with toluene and benzene allowed us to further increase the inner pore diameter of the nanospheres to 18−21 nm (see Supporting Information Table S1). Toluene has been reported earlier as a powerful swelling agent in organosilica synthesis,[63] but its superior performance for hollow sphere synthesis has not been reported earlier. It is

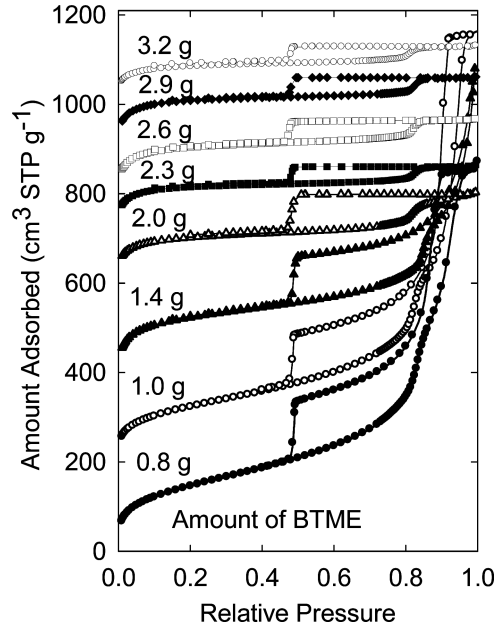

Figure 3. Nitrogen adsorption isotherms of ethylene-bridged organosilicas prepared with different relative amounts of BTME precursor (per 0.50 g F127). The adsorption isotherms were offset vertically by 200, 350, 600, 700, 770, 870, and 1000 cm^3 STP g^{-1} for materials synthesized using 1.0, 1.4, 2.0, 2.3, 2.6, 2.9, and 3.2 g of BTME, respectively.[73]

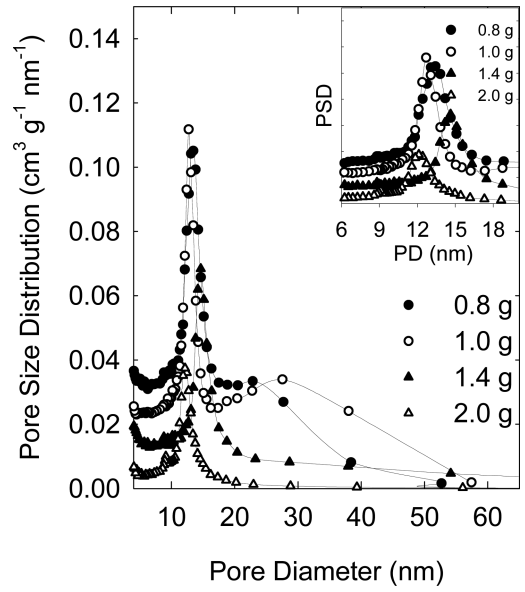

Figure 4. Pore size distributions of ethylene-bridged organosilicas prepared with different masses of BTME in the range 0.8−2 g (per 0.50 g F127).[73]

also noteworthy that in some cases, the pore size achieved for the isolated spheres was appreciably larger than that achieved for PMOs prepared under similar conditions.[62,63]

It was hypothesized that the organosilica (or silica) precursor (or products of its partial hydrolysis) is absorbed by the PEO-PPO-PEO micelles and distributed in the PEO coronas and on the interface between the PEO corona and PPO core[32,50] (or even solubilized in the hydrophobic core of the micelle, as hypothesized by others in the case of silica precursor[55]). There is evidence that the organosilica framework can approach the

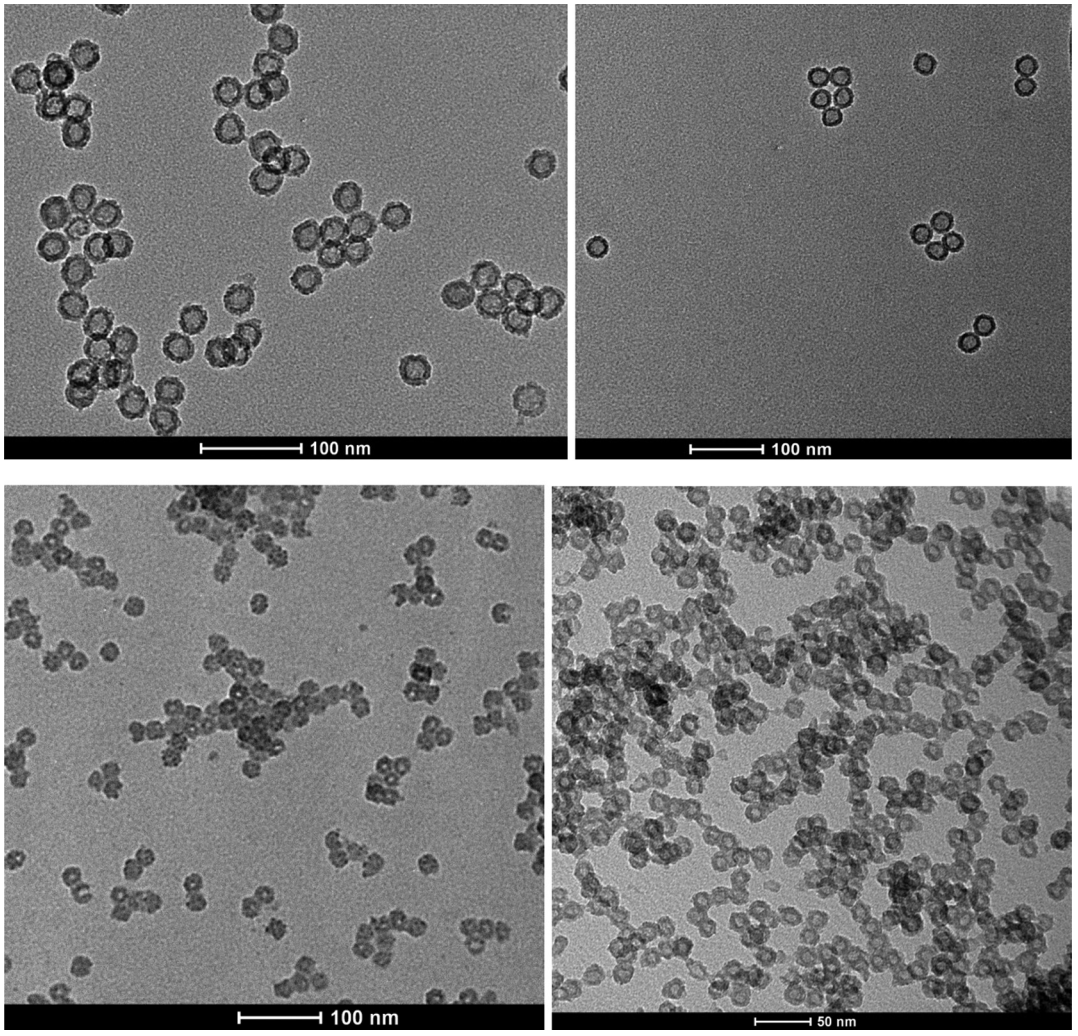

Figure 5. TEM images of hollow organosilica nanospheres with different bridging groups: (top left) methylene (−CH_2−), (top right), ethylene (−CH_2CH_2−), (bottom left), ethenylene (−CH═CH−), and (bottom right) phenylene (−C_6H_4−).[73]

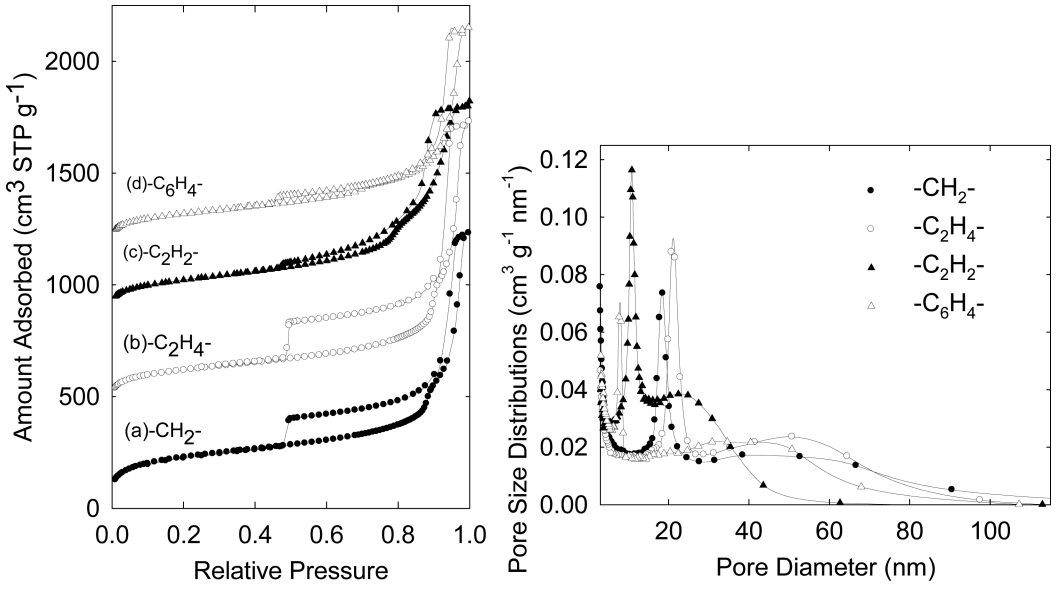

Figure 6. (left) Nitrogen adsorption isotherms and (right) pore size distributions for hollow organosilica nanospheres with methylene, ethylene, ethenylene, and phenylene bridging groups. The adsorption isotherms were offset vertically by 445, 880, and 1140 cm^3 STP g^{-1} for ethylene, ethenylene, and phenylene-bridged materials.[73]

dx.doi.org/10.1021/cm202136r | *Chem. Mater.* 2012, 24, 123−132

micelle core more closely than the silica framework in silica/$EO_mPO_nEO_m$ composites.[63,64] It is our hypothesis that if the relative amount of the organosilica precursor with respect to the PEO-PPO-PEO micelles is limited, the concentration of the precursor on the surface of the micelles is likely to be small and the cross-linking between the organosilica/micelle nanoparticles is hindered, thus preventing the precursor-filled micelles from consolidating into periodic structures or otherwise. On the basis of this hypothesis, the synthesis of hollow spheres of other compositions was performed and proved successful. As can be seen from TEM images in Figure 5, methylene-, ethenylene- and phenylene-bridged organosilicas in the form of hollow spheres were obtained. The structural perfection was the highest for methylene- and ethylene-bridged materials, while spheres of ethenylene- and phenylene-bridged organosilicas were rougher, and, in the former case, some of them had parts of their walls missing (Figure 5 and Supporting Figures S1–S2). It is noteworthy that for methylene- and phenylene-bridged organosilicas, the increase in the relative amount of the framework precursor did not render well-ordered consolidated structures (although weakly ordered PMO was reported earlier[62]), thus showing that the propensity to the formation of hollow organosilica nanospheres under the considered conditions was high. While phenylene-bridged organosilica nanospheres were reported by others,[50] we are not aware of a report on single-micelle-templated methylene- and ethenylene-bridged organosilica nanospheres.

The hollow spheres with a variety of compositions showed similar nitrogen adsorption isotherms (Figure 6) featuring a steep capillary condensation step at a relative pressure of 0.7–0.9 (depending on the composition and other synthesis conditions) followed by a major increase in uptake close to the saturation vapor pressure. The additional porosity, which is attributable to the voids between loosely packed spheres, was reflected on PSDs (see Figure 6). It is notable that the height of the capillary condensation step was the lowest for phenylene-bridged spheres, showing that they exhibit the lowest volume of the voids inside the spheres. Some of the hollow nanospheres reported herein exhibited exceptionally high pore diameter, reaching 18–21 nm for not only ethylene-bridged organosilicas but also methylene-bridged sample (Table S1). The combination of the high volume of the uniform mesopores and the large pore size makes these nanospheres very interesting materials for a variety of applications for which nanoscale hollow spheres are contemplated.[49,51,52] It is also noteworthy that in most cases, the capillary evaporation from the uniform mesopores appeared to be delayed to the lower limit of adsorption–desorption hysteresis (p/p_0 = ~0.48), indicating that the inner void spaces in the spherical particles were accessible from the surrounding through passages of diameter lower than 5 nm.[82] However, the capillary evaporation for the ethenylene-bridged silica took place primarily above the lower limit of hysteresis, indicating a larger size of entrances to the spherical voids. This is consistent with TEM, which showed substantial gaps in the walls of some particles (see Figure 5 and Supporting Information Figures S1–S2). The hollow nanospheres showed SAXS patterns similar to those discussed earlier in the context of ethylene-bridged organosilica nanospheres (see Figure 7).

The hollow nanospheres have a significant thermal stability. The bridging groups were burned out (converting organosilica to silica framework) with retention of narrow PSD, although the pore diameter decreased (Supporting Figure S3). This is similar to the recent report on the behavior of organosilica

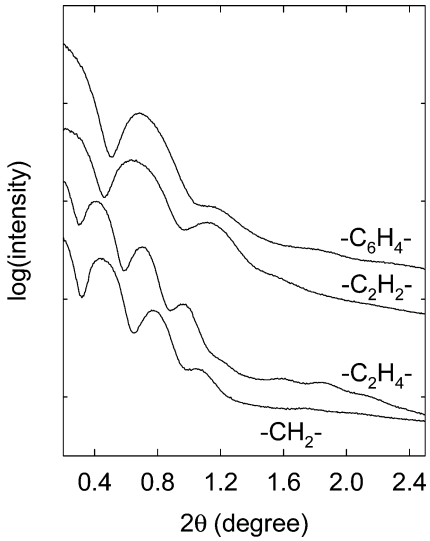

Figure 7. SAXS patterns of hollow organosilica nanospheres with methylene, ethylene, ethenylene, and phenylene bridging groups.[73]

nanotubes.[60] The inner spherical voids (see TEM in Supporting Figure S4) were accessible even after calcination at 500 °C under air, while related PMO was converted to closed-pore ordered mesoporous silica at 400 °C.[63] This result suggests that while ethylene-bridged PMOs are readily converted to closed-pore silicas, the formation of closed-pore silica nanospheres through the thermal treatment may be difficult. The larger pore wall thickness of the consolidated structures, expected on the basis of the higher BTME/F127 ratio, may play a major role in making them more amenable to the thermally induced pore closure.

It was attempted to use a silica precursor (TEOS) to directly synthesize hollow silica spheres by reducing TEOS/F127 ratio in the synthesis that affords LP-FDU-12 in the presence of xylenes as a swelling agent. However, we were unable to obtain any product with good structural integrity. It was hypothesized that organosilica precursors reside more deeply within the micelles, interacting with PEO corona and perhaps also with PPO blocks (especially on PEO/PPO boundary), whereas silica precursors form a thinner layer, primarily in the PEO corona, which may make a resulting silica wall less stable. To mimic the distribution of the framework precursor within the micelles, a block copolymer with a larger hydrophilic block (Pluronic F108) was used together with the silica precursor, hoping that it will lead to a thick layer of silica formed in the PEO corona of the micelles and render the desired hollow silica spheres. Indeed, the hollow silica product has been recovered (see TEM in Figure 8), which exhibited an adsorption isotherm similar to those discussed earlier for hollow sphere products and having the pore diameter ~23 nm, which is exceptionally large (see Figure 8).

The successful synthesis of hollow organosilica and silica nanospheres through the reduction of the framework-precursor/surfactant ratio prompted us to investigate the possibility of synthesizing hollow organosilica nanotubes. In this case, Pluronic P123 surfactant was used, as it is known to afford organosilicas templated by cylindrical micelles.[64,69] While the formation of nanotube products appeared to take place only under certain conditions, in contrast to the nanosphere formation that was readily achievable at low precursor/surfactant ratios, it was possible to obtain quite well-defined

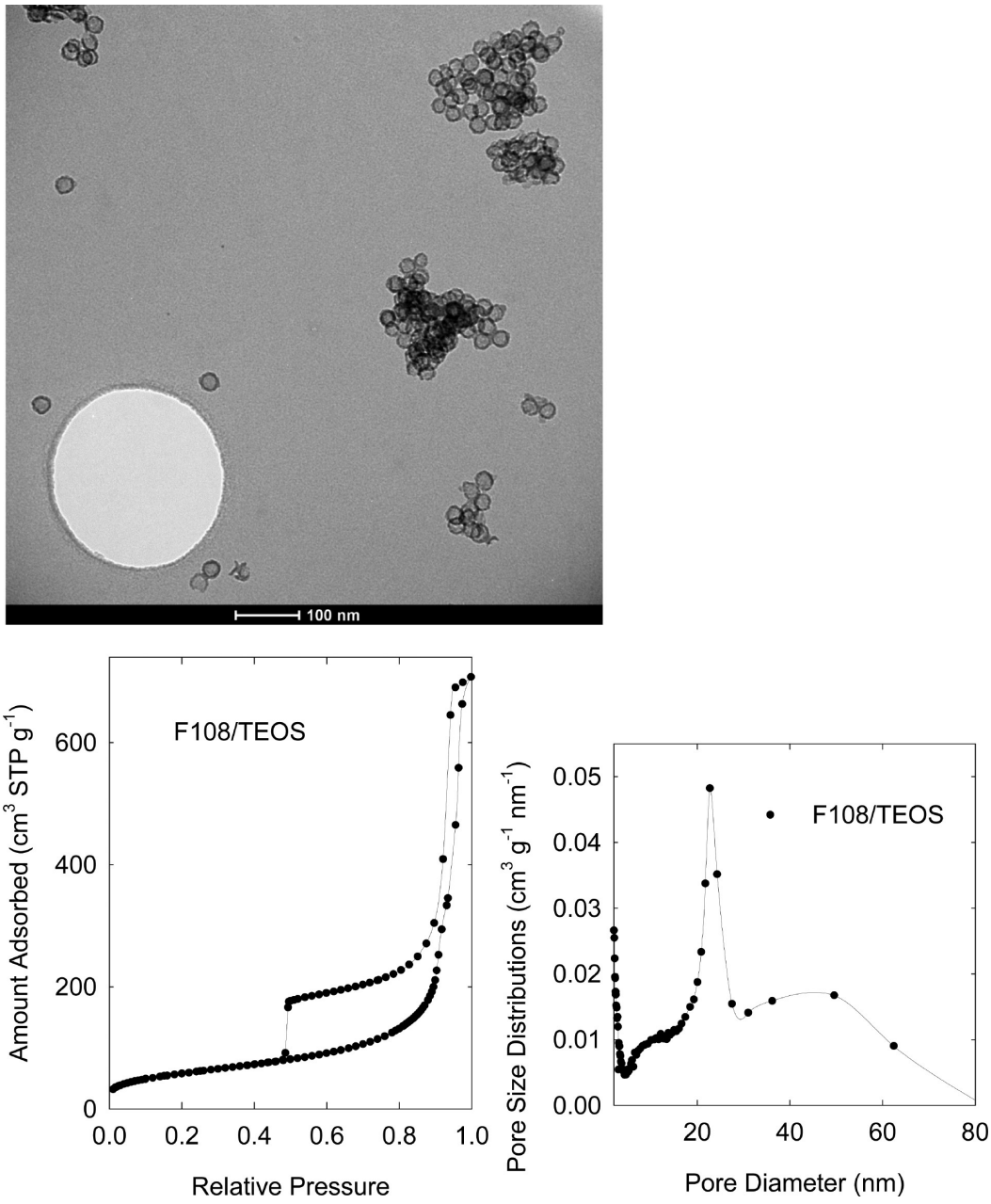

Figure 8. (top) TEM image, (bottom left) nitrogen adsorption isotherm, and (bottom right) pore size distribution of hollow silica nanospheres templated by Pluronic F108 triblock copolymer.[73]

nanotubes for ethylene-bridged organosilica (see TEM image in Figure 9). The nanotubes appeared to be slightly contaminated with hollow spheres. The formation of the nanotubes was facilitated by the presence of ammonium fluoride in the synthesis mixture. Apparently, a faster hydrolysis and condensation of the organosilica precursor was beneficial for the formation of the individual porous nanoparticles instead of consolidated porous structures. As in the case of hollow spheres, the adsorption isotherm (Figure 10) for the tube-like product featured a steep capillary condensation step followed by further increase in the amount adsorbed, which can be attributed to capillary condensation inside the tubes and multilayer adsorption combined with capillary condensation between the tubes, respectively. Others recently reported organosilica nanotubes, although with much lower pore diameters.[60] SAXS pattern of the hollow tubes (Figure 10) was not well resolved, as expected from TEM images showing low degree of structural ordering (if any).

Both nanospheres and nanotubes were aggregated to some extent. It is not clear at present to what extent these nanoobjects were covalently cross-linked. Others have reported approached to suppress the aggregation,[32,56,57,59] which are expected to be applicable to our materials.

As-synthesized and extracted or calcined products were analyzed by thermogravimetry to investigate the surfactant content. The weight loss was greatly diminished after the surfactant removal process, showing that the hollow nanoobjects were surfactant-templated. ^{29}Si NMR characterization showed that the extracted hollow spheres had intact bridging groups, while the calcined spheres suffered some Si−C bond cleavage (Supporting Information Figures S5−S8), which

dx.doi.org/10.1021/cm202136r | *Chem. Mater.* 2012, 24, 123−132

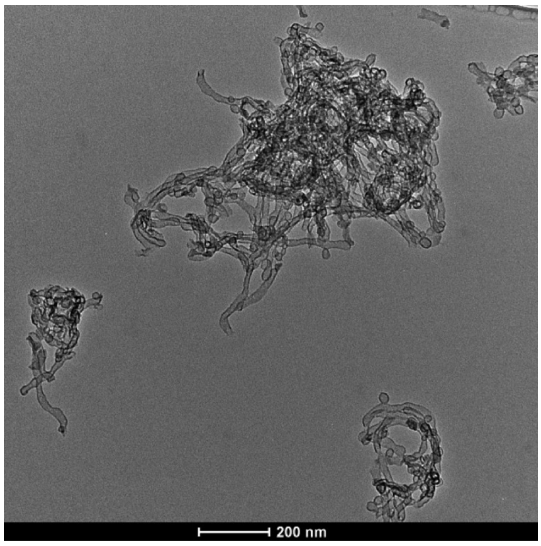

Figure 9. TEM image of ethylene-bridged organosilica nanotubes.[73]

typically can be eliminated through adjustment of calcination temperature and/or atmosphere or through extraction.[64]

CONCLUSIONS

In the case of organosilicas templated by spherical micelles of PEO-based block-copolymer surfactants, the lowering of the framework-precursor/surfactant ratio favors the formation of hollow nanoparticles templated by single micelles. This behavior may be related to the location of the framework precursor in the interior of the micelle (primarily in PEO corona) and its reduced ability to form cross-links between the precursor-filled micelles, if the relative amount of the precursor is sufficiently low. A proper adjustment of the framework-precursor/surfactant ratio allows one to obtain hollow organosilica nanospheres of different framework compositions, having aliphatic, unsaturated and aromatic bridging groups. The inner pore size of the nanospheres can be controlled using an appropriate micelle swelling agent from the family of benzene and its alkyl-substituted derivatives and reaches 20 nm for some framework compositions. The organosilica spheres can be converted to pure-silica spheres through calcination without the loss of intergrity and without thermally induced closing of the inner pore space. It was possible to extend our synthesis approach on the direct synthesis of pure silica nanospheres, but this was accomplished by selecting a block copolymer surfactant with a higher proportion of the hydrophilic blocks

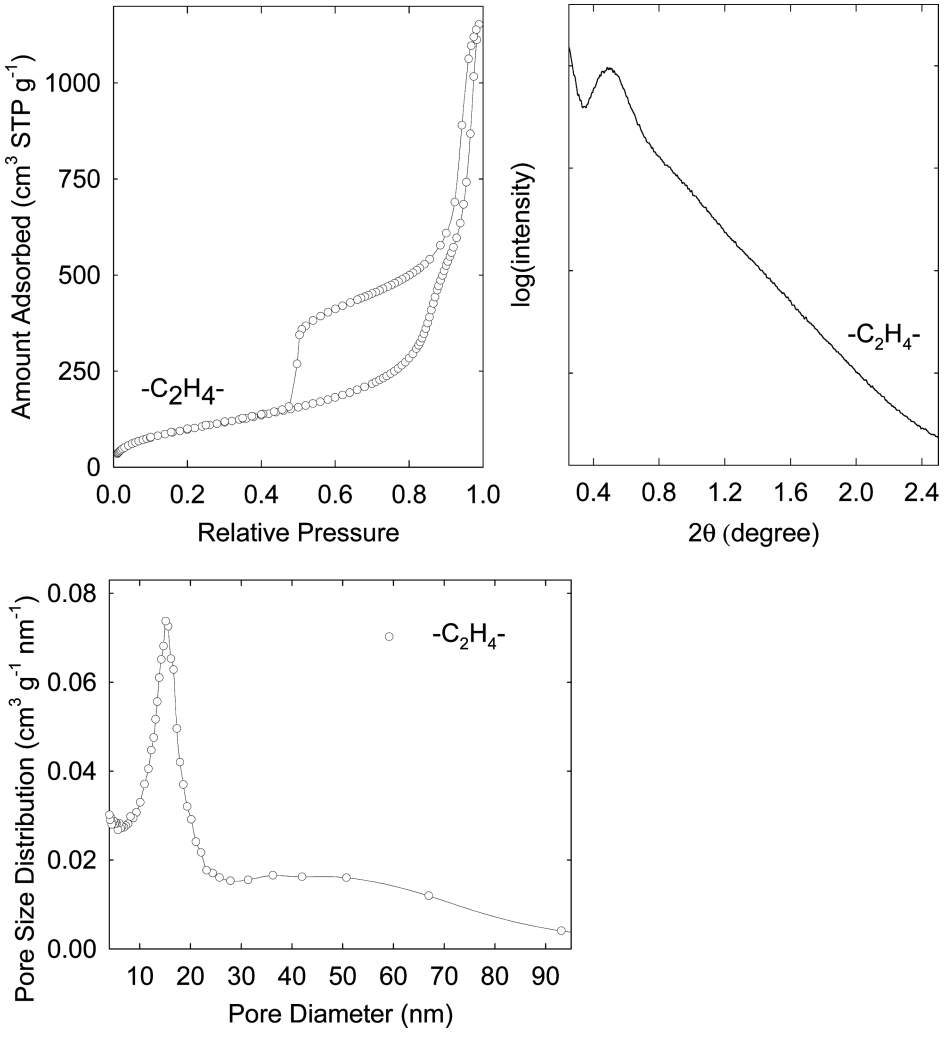

Figure 10. (top left) Nitrogen adsorption isotherm, (top right) SAXS pattern, and (bottom) pore size distribution of ethylene-bridged organosilica nanotubes.[73]

dx.doi.org/10.1021/cm202136r | *Chem. Mater.* 2012, 24, 123–132

than for the surfactant used for the organosilica nanosphere synthesis. The adjustment of the amount of the framework precursor relative to the surfactant allowed us to obtain organosilica nanotubes as well.

■ ASSOCIATED CONTENT

Supporting Information

Table with structural parameters derived from gas adsorption. Figures with adsorption isotherms and pore size distributions derived from them; TEM images and NMR spectra. This material is available free of charge via the Internet at http://pubs.acs.org.

■ AUTHOR INFORMATION

Corresponding Author

*E-mail: Michal.Kruk@csi.cuny.edu.

Present Address

[§]Department of Chemistry, Lehigh University, Bethlehem, PA 18015, USA.

■ ACKNOWLEDGMENTS

NSF is gratefully acknowledged for partial support of this research (award DMR-0907487) and for funding the acquisition of SAXS/WAXS system through award CHE-0723028. Acknowledgment is made to the Donors of the American Chemical Society Petroleum Research Fund for partial support of this research (Award PRF #49093-DNI5). The Imaging Facility at CSI is acknowledged for providing access to TEM. Professor Ruth Stark, Dr. Hsin Wang, and Dr. Subhasish Chatterjee (City College of New York) are gratefully acknowledged for help with NMR measurements. BASF is acknowledged for the donation of the block copolymers.

■ REFERENCES

(1) Alexandridis, P.; Alan Hatton, T. *Colloids Surf., A* **1995**, *96*, 1−46.
(2) Booth, C.; Attwood, D. *Macromol. Rapid Commun.* **2000**, *21*, 501−527.
(3) Beck, J. S.; Vartuli, J. C.; Roth, W. J.; Leonowicz, M. E.; Kresge, C. T.; Schmitt, K. D.; Chu, C. T. W.; Olson, D. H.; Sheppard, E. W.; McCullen, S. B.; Higgins, J. B.; Schlenker, J. L. *J. Am. Chem. Soc.* **1992**, *114*, 10834−10843.
(4) Inagaki, S.; Fukushima, Y.; Kuroda, K. *J. Chem. Soc., Chem. Commun.* **1993**, 680−682.
(5) Monnier, A.; Schueth, F.; Huo, Q.; Kumar, D.; Margolese, D.; Maxwell, R. S.; Stucky, G. D.; Krishnamurty, M.; Petroff, P.; Firouzi, A.; Janicke, M.; Chmelka, B. F. *Science* **1993**, *261*, 1299−1303.
(6) Huo, Q.; Margolese, D. I.; Ciesla, U.; Feng, P.; Gier, T. E.; Sieger, P.; Leon, R.; Petroff, P. M.; Schueth, F.; Stucky, G. D. *Nature* **1994**, *368*, 317−321.
(7) Zhao, D.; Huo, Q.; Feng, J.; Chmelka, B. F.; Stucky, G. D. *J. Am. Chem. Soc.* **1998**, *120*, 6024−6036.
(8) Kresge, C. T.; Leonowicz, M. E.; Roth, W. J.; Vartuli, J. C.; Beck, J. S. *Nature* **1992**, *359*, 710−712.
(9) Schueth, F. *Chem. Mater.* **2001**, *13*, 3184−3195.
(10) Davis, M. E. *Nature* **2002**, *417*, 813−821.
(11) Hoffmann, F.; Cornelius, M.; Morell, J.; Froeba, M. *Angew. Chem., Int. Ed.* **2006**, *45*, 3216−3251.
(12) Wan, Y.; Zhao, D. *Chem. Rev.* **2007**, *107*, 2821−2860.
(13) Kramer, E.; Forster, S.; Goltner, C.; Antonietti, M. *Langmuir* **1998**, *14*, 2027−2031.
(14) Bagshaw, S. A.; Prouzet, E.; Pinnavaia, T. J. *Science* **1995**, *269*, 1242−1244.
(15) Attard, G. S.; Glyde, J. C.; Goltner, C. G. *Nature* **1995**, *378*, 366−368.
(16) Tanev, P. T.; Pinnavaia, T. J. *Science* **1995**, *267*, 865−867.
(17) Wanka, G.; Hoffmann, H.; Ulbricht, W. *Macromolecules* **1994**, *27*, 4145−4149.
(18) Almgren, M.; Brown, W.; Hvidt, S. *Colloid Polym. Sci.* **1995**, *273*, 2−15.
(19) Melosh, N. A.; Lipic, P.; Bates, F. S.; Wudl, F.; Stucky, G. D.; Fredrickson, G. H.; Chmelka, B. F. *Macromolecules* **1999**, *32*, 4332−4342.
(20) de Paul, S. M.; Zwanziger, J. W.; Ulrich, R.; Wiesner, U.; Spiess, H. W. *J. Am. Chem. Soc.* **1999**, *121*, 5727−5736.
(21) Ryoo, R.; Ko, C. H.; Kruk, M.; Antochshuk, V.; Jaroniec, M. *J. Phys. Chem. B* **2000**, *104*, 11465−11471.
(22) Kruk, M.; Jaroniec, M.; Joo, S. H.; Ryoo, R. *J. Phys. Chem. B* **2003**, *107*, 2205−2213.
(23) Choi, M.; Heo, W.; Kleitz, F.; Ryoo, R. *Chem. Commun.* **2003**, 1340−1341.
(24) Van Der Voort, P.; Ravikovitch, P. I.; De Jong, K. P.; Benjelloun, M.; Van Bavel, E.; Janssen, A. H.; Neimark, A. V.; Weckhuysen, B. M.; Vansant, E. F. *J. Phys. Chem. B* **2002**, *106*, 5873−5877.
(25) Caruso, F.; Caruso, R. A.; Moehwald, H. *Science* **1998**, *282*, 1111−1114.
(26) Yuan, J.-J.; Mykhaylyk, O. O.; Ryan, A. J.; Armes, S. P. *J. Am. Chem. Soc.* **2007**, *129*, 1717−1723.
(27) Liu, J.; Yang, Q.; Zhang, L.; Yang, H.; Gao, J.; Li, C. *Chem. Mater.* **2008**, *20*, 4268−4275.
(28) Lee, H.; Char, K. *ACS Appl. Mater. Interfaces* **2009**, *1*, 913−920.
(29) Tang, J.; Liu, J.; Wang, P.; Zhong, H.; Yang, Q. *Microporous Mesoporous Mater.* **2010**, *127*, 119−125.
(30) Du, L.; Liao, S.; Khatib, H. A.; Stoddart, J. F.; Zink, J. I. *J. Am. Chem. Soc.* **2009**, *131*, 15136−15142.
(31) Corma, A.; Díaz, U.; Arrica, M.; Fernández, E.; Ortega, Í. *Angew. Chem., Int. Ed.* **2009**, *48*, 6247−6250.
(32) Huo, Q.; Liu, J.; Wang, L.-Q.; Jiang, Y.; Lambert, T. N.; Fang, E. *J. Am. Chem. Soc.* **2006**, *128*, 6447−6453.
(33) Tang, J.; Zhou, X.; Zhao, D.; Lu, G. Q.; Zou, J.; Yu, C. *J. Am. Chem. Soc.* **2007**, *129*, 9044−9048.
(34) Khanal, A.; Inoue, Y.; Yada, M.; Nakashima, K. *J. Am. Chem. Soc.* **2007**, *129*, 1534−1535.
(35) Jan, J.-S.; Lee, S.; Carr, C. S.; Shantz, D. F. *Chem. Mater.* **2005**, *17*, 4310−4317.
(36) Djojoputro, H.; Zhou, X. F.; Qiao, S. Z.; Wang, L. Z.; Yu, C. Z.; Lu, G. Q. *J. Am. Chem. Soc.* **2006**, *128*, 6320−6321.
(37) Cao, A.; Ye, Z.; Cai, Z.; Dong, E.; Yang, X.; Liu, G.; Deng, X.; Wang, Y.; Yang, S.-T.; Wang, H.; Wu, M.; Liu, Y. *Angew. Chem., Int. Ed.* **2010**, *49*, 3022−3025.
(38) Jiang, X.; Ward, T. L.; Cheng, Y.-S.; Liu, J.; Brinker, C. J. *Chem. Commun.* **2010**, 3019−3021.
(39) Sun, Z.; Bai, F.; Wu, H.; Schmitt, S. K.; Boye, D. M.; Fan, H. *J. Am. Chem. Soc.* **2009**, *131*, 13594−13595.
(40) Tan, B.; Vyas, S. M.; Lehmler, H.-J.; Knutson, B. L.; Rankin, S. E. *Adv. Funct. Mater.* **2007**, *17*, 2500−2508.
(41) Liu, J.; Qiao, S. Z.; Hartono, S. B.; Lu, G. Q. *Angew. Chem., Int. Ed.* **2010**, *49*, 4981−4985.
(42) Holmstrom, S. C.; King, P. J. S.; Ryadnov, M. G.; Butler, M. F.; Mann, S.; Woolfson, D. N. *Langmuir* **2008**, *24*, 11778−11783.
(43) Lei, S.; Zhang, J.; Wang, J.; Huang, J. *Langmuir* **2009**, *26*, 4288−4295.
(44) Yuwono, V. M.; Hartgerink, J. D. *Langmuir* **2007**, *23*, 5033−5038.
(45) Chen, X.; Berger, A.; Ge, M.; Hopfe, S.; Dai, N.; Gösele, U.; Schlecht, S.; Steinhart, M. *Chem. Mater.* **2011**, *23*, 3129−3131.
(46) Kang, D.-Y.; Zang, J.; Wright, E. R.; McCanna, A. L.; Jones, C. W.; Nair, S. *ACS Nano* **2010**, *4*, 4897−4907.
(47) Feng, Z.; Li, Y.; Niu, D.; Li, L.; Zhao, W.; Chen, H.; Li, L.; Gao, J.; Ruan, M.; Shi, J. *Chem. Commun.* **2008**, 2629−2631.
(48) Harada, M.; Adachi, M. *Adv. Mater.* **2000**, *12*, 839−841.
(49) Hao, N.; Wang, H.; Webley, P. A.; Zhao, D. *Microporous Mesoporous Mater.* **2010**, *132*, 543−551.
(50) Liu, J.; Bai, S.; Zhong, H.; Li, C.; Yang, Q. *J. Phys. Chem. C* **2010**, *114*, 953−961.

(51) Gao, J.; Liu, J.; Bai, S.; Wang, P.; Zhong, H.; Yang, Q.; Li, C. *J. Mater. Chem.* **2009**, *19*, 8580−8588.
(52) Gao, J.; Liu, J.; Tang, J.; Jiang, D.; Li, B.; Yang, Q. *Chem.—Eur. J.* **2010**, *16*, 7852−7858.
(53) Koh, K.; Ohno, K.; Tsujii, Y.; Fukuda, T. *Angew. Chem., Int. Ed.* **2003**, *42*, 4194−4197.
(54) Liu, D.; Sasidharan, M.; Nakashima, K. *J. Colloid Interface Sci.* **2011**, *358*, 354−359.
(55) Tan, H.; Liu, N. S.; He, B.; Wong, S. Y.; Chen, Z.-K.; Li, X.; Wang, J. *Chem. Commun.* **2009**, 6240−6242.
(56) Zhu, J.; Tang, J.; Zhao, L.; Zhou, X.; Wang, Y.; Yu, C. *Small* **2010**, *6*, 276−282.
(57) Chi, F.; Guan, B.; Yang, B.; Liu, Y.; Huo, Q. *Langmuir* **2010**, *26*, 11421−11426.
(58) Chi, F.; Guo, Y.-N.; Liu, J.; Liu, Y.; Huo, Q. *J. Phys. Chem. C* **2010**, *114*, 2519−2523.
(59) Qiao, Z.-A.; Dai, T.; Liu, Y.; Huo, Q. *J. Colloid Interface Sci.* **2010**, *352*, 401−404.
(60) Liu, X.; Li, X.; Guan, Z.; Liu, J.; Zhao, J.; Yang, Y.; Yang, Q. *Chem. Commun.* **2011**, *47*, 8073−8075.
(61) Ding, S.; Liu, N.; Li, X.; Peng, L.; Guo, X.; Ding, W. *Langmuir* **2010**, *26*, 4572−4575.
(62) Kruk, M.; Hui, C. M. *J. Am. Chem. Soc.* **2008**, *130*, 1528−1529.
(63) Mandal, M.; Kruk, M. *J. Phys. Chem. C* **2010**, *114*, 20091−20099.
(64) Mandal, M.; Kruk, M. *J. Mater. Chem.* **2010**, *20*, 7506−7516.
(65) Foulias, K. Senior Honors Thesis, College of Staten Island, 2008.
(66) Inagaki, S.; Guan, S.; Fukushima, Y.; Ohsuna, T.; Terasaki, O. *J. Am. Chem. Soc.* **1999**, *121*, 9611−9614.
(67) Melde, B. J.; Holland, B. T.; Blanford, C. F.; Stein, A. *Chem. Mater.* **1999**, *11*, 3302−3308.
(68) Asefa, T.; MacLachlan, M. J.; Coombs, N.; Ozin, G. A. *Nature* **1999**, *402*, 867−871.
(69) Zhu, H.; Jones, D. J.; Zajac, J.; Roziere, J.; Dutartre, R. *Chem. Commun.* **2001**, 2568−2569.
(70) Muth, O.; Schellbach, C.; Froeba, M. *Chem. Commun.* **2001**, 2032−2033.
(71) Matos, J. R.; Kruk, M.; Mercuri, L. P.; Jaroniec, M.; Asefa, T.; Coombs, N.; Ozin, G. A.; Kamiyama, T.; Terasaki, O. *Chem. Mater.* **2002**, *14*, 1903−1905.
(72) Zhou, X.; Qiao, S.; Hao, N.; Wang, X.; Yu, C.; Wang, L.; Zhao, D.; Lu, G. Q. *Chem. Mater.* **2007**, *19*, 1870−1876.
(73) Mandal, M. Ph.D. Dissertation, City University of New York, 2010.
(74) Huang, L.; Yan, X.; Kruk, M. *Langmuir* **2010**, *26*, 14871−14878.
(75) Sing, K. S. W.; Everett, D. H.; Haul, R. A. W.; Moscou, L.; Pierotti, R. A.; Rouquerol, J.; Siemieniewska, T. *Pure Appl. Chem.* **1985**, *57*, 603−619.
(76) Barrett, E. P.; Joyner, L. G.; Halenda, P. P. *J. Am. Chem. Soc.* **1951**, *73*, 373−380.
(77) Kruk, M.; Jaroniec, M.; Sayari, A. *Langmuir* **1997**, *13*, 6267−6273.
(78) Kruk, M.; Hui, C. M. *Microporous Mesoporous Mater.* **2008**, *114*, 64−73.
(79) Matos, J. R.; Kruk, M.; Mercuri, L. P.; Jaroniec, M.; Zhao, L.; Kamiyama, T.; Terasaki, O.; Pinnavaia, T. J.; Liu, Y. *J. Am. Chem. Soc.* **2003**, *125*, 821−829.
(80) Ravikovitch, P. I.; Neimark, A. V. *Langmuir* **2002**, *18*, 1550−1560.
(81) Jaroniec, M.; Kruk, M.; Olivier, J. P. *Langmuir* **1999**, *15*, 5410−5413.
(82) Kruk, M.; Jaroniec, M. *Chem. Mater.* **2003**, *15*, 2942−2949.